Received: 15 July 2020 | Revised: 27 October 2020 | Accepted: 31 October 2020

DOI: 10.1002/ardp.202000237

FULL PAPER

ARCH PHARM DPhG Archiv der Pharmazie

Design and discovery of new 1,2,4-triazolo[4,3-*c*]quinazolines as potential DNA intercalators and topoisomerase II inhibitors

Mohamed S. Alesawy[1] | Ahmed A. Al-Karmalawy[2] | Eslam B. Elkaeed[3] | Mohamed Alswah[3] | Ahmed Belal[4] | Mohammed S. Taghour[1] | Ibrahim H. Eissa[1]

[1]Pharmaceutical Medicinal Chemistry and Drug Design Department, Faculty of Pharmacy (Boys), Al-Azhar University, Cairo, Egypt

[2]Department of Pharmaceutical Medicinal Chemistry, Faculty of Pharmacy, Horus University-Egypt, New Damietta, Egypt

[3]Department of Pharmaceutical Organic Chemistry, Faculty of Pharmacy (Boys), Al-Azhar University, Cairo, Egypt

[4]Zoology Department, Faculty of Science, Al-Azhar University, Cairo, Egypt

Correspondence

Ibrahim H. Eissa and Mohamed S. Alesawy, Pharmaceutical Medicinal Chemistry and Drug Design Department, Faculty of Pharmacy (Boys), Al-Azhar University, Cairo 11884, Egypt.

Email: Ibrahimeissa@azhar.edu.eg (I. H. E.) and mohammedalesawy@azhar.edu.eg (M. S. A.)

Abstract

A new series of 1,2,4-triazolo[4,3-*c*]quinazoline derivatives was designed and synthesized as Topo II inhibitors and DNA intercalators. The cytotoxic effect of the new members was evaluated in vitro against a group of cancer cell lines including HCT-116, HepG-2, and MCF-7. Compounds **14$_c$**, **14$_d$**, **14$_e$**, **14$_e$**, **15$_b$**, **18$_b$**, **18$_c$**, and **19$_b$** exhibited the highest activities with IC_{50} values ranging from 5.22 to 24.24 μM. Furthermore, Topo II inhibitory activities and DNA intercalating affinities of the most promising candidates were evaluated as a possible mechanism for the antiproliferative effect. The results of the Topo II inhibition and DNA binding tests were coherent with that of in vitro cytotoxicity. Additionally, the most promising compound **18$_c$** was analyzed in HepG-2 cells for its apoptotic effect and cell cycle arrest. It was found that **18$_c$** can induce apoptosis and arrest the cell cycle at the G2–M phase. Finally, molecular docking studies were carried out for the designed compounds against the crystal structure of the DNA–Topo II complex as a potential target to explore their binding modes. On the basis of these studies, it was hypothesized that the DNA binding and/or Topo II inhibition would participate in the noted cytotoxicity of the synthesized compounds.

KEYWORDS

anticancer, DNA intercalator, molecular docking, 1,2,4-triazolo[4,3-c]quinazoline, topoisomerase II

1 | INTRODUCTION

Cancer is a serious public health issue in all countries[1] and it marks its beginning when cells begin to grow without control in a part of the body.[2] According to WHO, cancer is the second leading cause of death worldwide, which accounted for an approximated 9.6 million deaths in 2018. Around one in six deaths worldwide are due to cancer.[3] Millions of people are still alive with cancer.[4] There are currently over 100 types of cancer, needing a particular diagnosis and treatment.[3] Compounds that interfere with DNA play a significant role in possible approaches to antitumor activity.[5] Many of these drugs demonstrate their antitumor activity by binding to DNA and/or enzymes essential to normal DNA functions, causing a cellular response that ultimately results in cell death.[6]

DNA intercalators are substances that bind with the helix of DNA via an intercalation process that causes cell cycle disruption and cell death.[7] The process of intercalation can be identified as the process by which molecules comprising planar aromatic or heteroaromatic ring systems, known as chromophores, are inserted into opposing DNA helix base pairs.[8] In addition, most intercalating agents are either positively charged or contain basic groups that under physiological conditions can be protonated.[6] DNA intercalators in clinical use include acridine

derivatives (e.g., amsacrine **1**),[8] anthracyclines (e.g., doxorubicin **2**, mitoxantrone **3**, and nogalamycin **5**),[9,10] and ellipticine $\mathbf{4_a}$.[11]

Topoisomerase II (Topo II) is a primary regulator of DNA replication.[12] Topo II modifies the topology of DNA, monitors the supercoiling of DNA, and controls a variety of critical nuclear mechanisms, such as transcription, replication, and repair.[13] It is possible to classify compounds targeting Topo II into two groups. The first is Topo II poisons, which increase the rate of cleavable complexes of Topo II–DNA, resulting in a lesion in DNA strands.[14] Topo II poisons include many clinically active compounds including doxorubicin **2**[9] and mitoxantrone **3**.[10] The second class inhibits the catalytic activity of Topo II without increasing the rates of the cleavable complexes of Topo II. The second class is known as catalytic inhibitors such as etoposide.[15] Targeting DNA and blocking Topo II are, therefore, effective strategies to find new anticancer agents.[16–26]

There are three common essential pharmacophoric features of DNA intercalators and Topo II poisons. The first is a polyaromatic planar structure (chromophore) sandwiched between base pairs of DNA.[27] The second feature is a cationic species, interacting with the negatively charged phosphate group of DNA. The cationic center may be an amino or nitrogen-containing heterocyclic group, which can be protonated at physiological pH.[7] The third feature is a groove-binding side chain moiety, which occupies the minor groove of DNA (Figure 1).[28–30]

Quinazoline is a substantial scaffold and one of the most promising classes of heterocycles that is well-tolerated in humans and possesses anticancer activity.[31–34] It is also the basis of many bioactive compounds that show potential activities as DNA intercalators and Topo inhibitors.[35,36] It has been documented that quinazoline analogs such as EBE-A22 **6** possess a DNA intercalating activity.[37] It has also been confirmed that several new moieties as triazole,[38] benzylidene,[39] and thiosemicarbazide[40] have antitumor activities.

1.1 | Rationale of molecular design

In continuation of our previous efforts of design and synthesis of new anticancer agents,[41–48] especially DNA intercalators and Topo II inhibitors,[14,49–51] ligand-based drug design approach was considered. Accordingly, molecular hybridization of quinazoline and other effective antitumor moieties was performed to obtain more

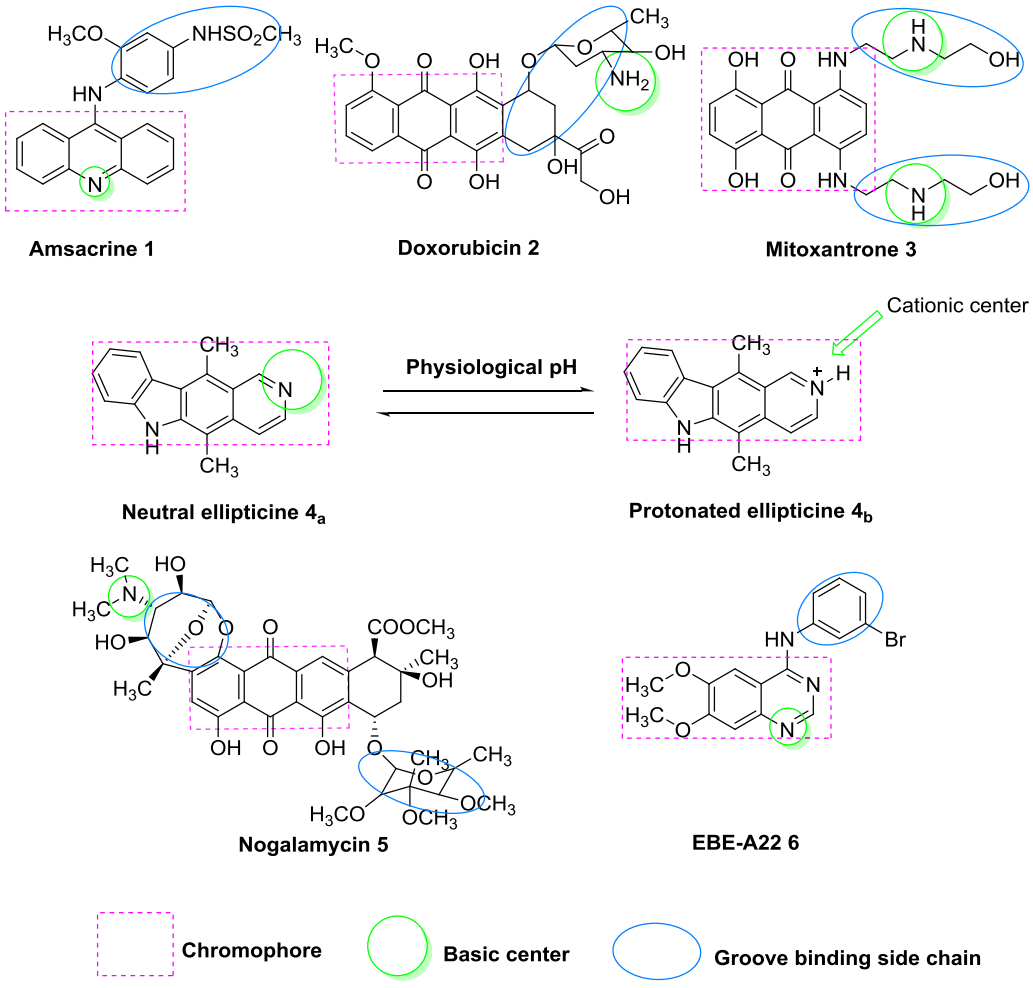

FIGURE 1 Some reported DNA intercalators and Topo II inhibitors exhibiting the essential pharmacophoric features

promising anticancer agents. The new compounds were designed to have the essential pharmacophoric features of DNA intercalators and Topo II inhibitors.

The rationale of our molecular design depended on the generation of the planar aromatic system, 1,2,4-triazolo[4,3-*c*]quinazoline (chromophore). Different groove-binding side chains were incorporated into the planar system at position-5. The side chains may be aliphatic or aromatic amines to generate the basic center (Supporting Information Data).

2 | RESULTS AND DISCUSSION

2.1 | Chemistry

The procedures of the synthesis of the target compounds are illustrated in Scheme 1. First, commercially available 2-aminobenzoic acid **7** was condensed with urea **8** at 200°C for 6 h to get quinazoline-2,4-dione **9** as white crystals.[52] Compound **9** was further treated with phosphorus oxychloride in the presence of triethylamine for 7 h to provide 2,4-dichloroquinazoline **10**.[53] 2-Chloro-4-hydrazinylquinazoline **11** was obtained by adding hydrazine hydrate dropwise to the alcoholic solution of 2,4-dichloro quinazoline **10**.[54] Subsequently, compound **11** reacted with triethyl orthoformate at 100°C for 1 h to afford 5-chloro-[1,2,4]triazolo[4,3-*c*] quinazoline **12**.[55] Compound **12** was heated with hydrazine hydrate to afford 5-hydrazinyl-[1,2,4]triazolo[4,3-*c*]quinazoline **13**. The infrared (IR) spectrum of compound **13** demonstrated stretching bands at 3,302 and 3,257 cm^{-1}, corresponding to NH_2 and NH groups, respectively. Moreover, the ^1H NMR (nuclear magnetic resonance) spectrum of this compound showed exchangeable signals at δ 4.68 and 9.30 ppm, corresponding to NH_2 and NH groups, respectively.

Reflux of **12** with commercially available alkyl amines, namely ethylamine, *n*-propylamine, *n*-pentylamine, cyclopentylamine, and diethylamine, in isopropyl alcohol (IPA) afforded the target compounds $\mathbf{14_{a–e}}$, respectively. The IR spectra of $\mathbf{14_{a–d}}$ demonstrated stretching bands at a range of 3,212–3,279 cm^{-1}, corresponding to NH groups. Moreover, ^1H NMR spectrum of these compounds showed exchangeable singlet signals at a range of δ 7.82–8.09 ppm, corresponding to NH groups. In addition, reflux of **12** with commercially available aromatic amines, namely 4-methylaniline, 4-aminobenzoic acid, and ethyl *p*-aminobenzoate, in IPA afforded the title compounds $\mathbf{15_{a–c}}$, respectively. The IR spectra of $\mathbf{15_{a–c}}$ showed stretching bands at a range of 3137–3189 cm^{-1}, corresponding to the NHs. Moreover, the ^1H NMR spectra of these compounds demonstrated exchangeable singlet signals at a range of δ 10.40–10.44 ppm, corresponding to NH groups. The reaction of compound **12** with benzylamine and morpholine in IPA produced compounds **16** and **17**, respectively.

Condensation of compound **13** with certain aromatic aldehydes, namely, 4-methylbenzaldehehyde, 4-nitrobenzaldehehyde, 4-hydroxybenzaldehehyde, and 2,6-dichlorobenzaldehehyde, in absolute ethanol with a catalytic amount of glacial acetic acid yielded the corresponding hydrazones $\mathbf{18_{a–d}}$, respectively. The ^1H NMR spectra of compounds $\mathbf{18_{a–d}}$ revealed the presence of D_2O-exchangeable singlet signals of hydrazinyl NH at a range of δ 9.80–11.53 ppm and singlet signals for the idene moiety at a range of δ 8.34–8.71 ppm.

Finally, target compounds $\mathbf{19_{a–d}}$ were synthesized by the reaction of **13** with appropriate isothiocyanates, namely, ethyl isothiocyanate, propyl isothiocyanate, butyl isothiocyanate, and phenyl isothiocyanate, in absolute ethanol. The IR spectra of compounds $\mathbf{19_{a–d}}$ showed sharp absorption bands of three NH groups of thiosemicarbazide moieties in the range of 3,173–3,205 cm^{-1}. The ^1H NMR spectrum of compound $\mathbf{19_b}$, as a representative example, showed three exchangeable singlet broad signals at around δ 8.24, 9.55, and 10.21 ppm, corresponding to the three NH groups.

2.2 | Biological testing

2.2.1 | In vitro antiproliferative activities

The synthesized compounds were evaluated for their cytotoxic activities against a group of cancer cell lines: colorectal carcinoma (HCT-116), hepatocellular carcinoma (HepG-2), and breast cancer (MCF-7). The standard 3-(4,5-dimethylthiazol-2-yl)-5-(3-carboxymethoxyphenyl)-2-(4-sulfophenyl)-2*H*-tetrazolium (MTT) method was used in this test,[56–58] utilizing doxorubicin as a positive control. The IC_{50} values are summarized in Table 1.

The results demonstrated that some of the tested compounds showed promising antiproliferative activities against the tested cells. In general, compounds $\mathbf{14_c}$, $\mathbf{14_d}$, $\mathbf{14_e}$, $\mathbf{15_b}$, $\mathbf{18_b}$, $\mathbf{18_c}$, and $\mathbf{19_b}$ exhibited good antiproliferative activities.

In particular, compound $\mathbf{18_c}$ was the most cytotoxic member and exhibited superior antiproliferative activities against HCT-116 and HepG-2 with IC_{50} values of 5.22 and 4.43 μM, respectively, compared with doxorubicin (IC_{50} = 9.63 and 8.28 μM, respectively). Also, compound $\mathbf{14_d}$ showed a higher activity than doxorubicin against HCT-116 (IC_{50} = 9.39 μM). In addition, compound $\mathbf{14_e}$ exhibited a higher activity than doxorubicin against HepG-2 with an IC_{50} value of 6.92 μM.

Compounds **13**, $\mathbf{14_d}$, $\mathbf{14_e}$, $\mathbf{15_b}$, $\mathbf{18_b}$, $\mathbf{18_c}$, and $\mathbf{19_b}$ showed strong antiproliferative activities against all tested cells with IC_{50} values ranging from 4.43 to 20.53 μM.

Compounds **14c** and $\mathbf{19_c}$ showed strong activities against only HCT-116 and HepG-2 cells with IC_{50} values ranging from 9.79 to 14.52 μM, whereas compounds $\mathbf{18_a}$ and $\mathbf{19_a}$ showed strong activities against only HepG-2 cells with IC_{50} values of 13.16 and 16.04 μM, respectively.

Moreover, compounds $\mathbf{14_a}$, $\mathbf{14_b}$, $\mathbf{15_a}$, $\mathbf{15_c}$, **16**, **17**, and 19_d showed moderate antiproliferative activities against HCT-116 and HepG-2 with IC_{50} values ranging from 20.41 to 38.78 μM, whereas compounds **13**, $\mathbf{14_c}$, $\mathbf{18_a}$, $\mathbf{19_a}$, and $\mathbf{19_c}$ showed moderate activities against MCF-7 with IC_{50} values of 22.72, 24.24, 27.28, 29.65, and 23.27 μM, respectively.

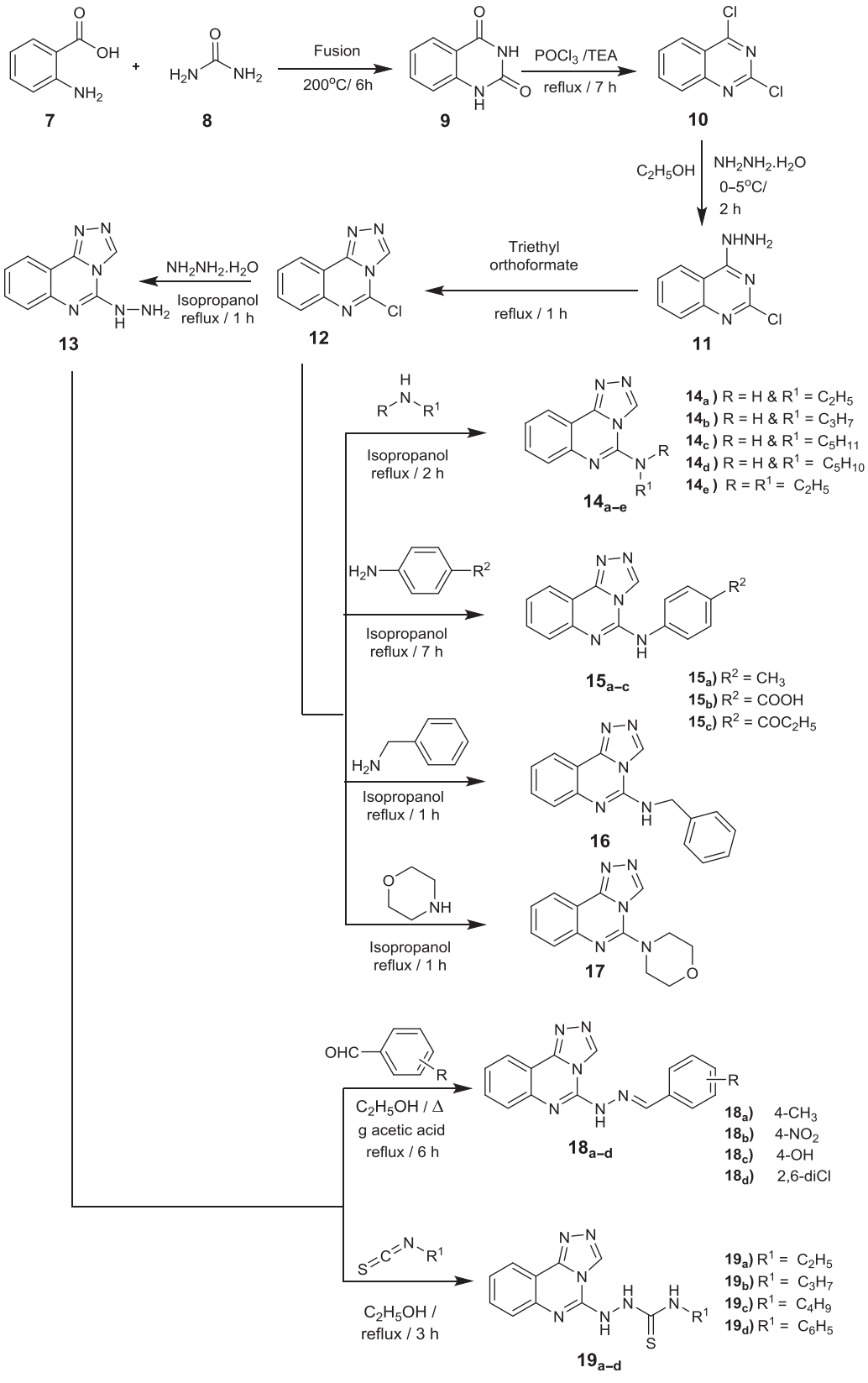

SCHEME 1 The general procedure for preparation of the target compounds

TABLE 1 In vitro antiproliferative activities against HCT-116, HepG-2, and MCF-7 cell lines, Topo II inhibitory activity, and DNA intercalating affinity of the synthesized compounds

Compound	Antiproliferative activities, IC_{50} (μM)[ab]			Topo II inhibition, IC_{50} (μM)[a]	DNA binding, IC_{50} (μM)[a]
	HCT-116	HepG-2	MCF-7		
13	14.23 ± 1.1	18.03 ± 1.3	22.72 ± 1.6	NT	NT
14_a	38.78 ± 2.2	29.87 ± 2.1	NA	NT	NT
14_b	28.02 ± 1.9	30.88 ± 2.3	NA	NT	NT
14_c	12.49 ± 0.4	9.79 ± 0.5	24.24 ± 1.7	1.93 ± 0.1	59.13 ± 3.1
14_d	9.39 ± 0.4	9.00 ± 0.4	13.50 ± 0.6	1.05 ± 0.1	54.52 ± 2.7
14_e	18.56 ± 1.2	6.92 ± 0.3	17.23 ± 1.1	1.78 ± 0.1	74.18 ± 5.2
15_a	27.34 ± 1.7	29.45 ± 2.1	48.12 ± 3.2	NT	NT
15_b	17.32 ± 0.9	11.66 ± 1.1	19.81 ± 1.2	3.51 ± 0.2	72.57 ± 4.8
15_c	37.46 ± 2.0	31.40 ± 2.4	NA	NT	NT
16	33.23 ± 1.9	20.41 ± 1.8	NA	NT	NT
17	33.96 ± 1.7	28.04 ± 1.9	48.33 ± 2.8	NT	NT
18_a	20.73 ± 1.1	13.16 ± 0.4	27.28 ± 1.5	2.78 ± 0.2	66.39 ± 3.6
18_b	12.84 ± 0.7	12.63 ± 0.5	15.42 ± 1.2	2.39 ± 0.2	67.35 ± 4.1
18_c	5.22 ± 0.3	4.43 ± 0.1	12.22 ± 1.0	0.86 ± 0.1	48.53 ± 3.2
18_d	43.17 ± 2.9	49.01 ± 3.2	NA	NT	NT
19_a	21.82 ± 0.7	16.04 ± 0.9	29.65 ± 1.7	4.67 ± 0.3	82.04 ± 6.5
19_b	18.11 ± 1.1	12.44 ± 0.5	20.53 ± 1.4	3.45 ± 0.3	79.63 ± 5.7
19_c	14.52 ± 0.5	12.93 ± 0.3	23.27 ± 1.8	NT	NT
19_d	34.25 ± 2.3	36.97 ± 2.1	43.47 ± 3.1	NT	NT
Doxorubicin	9.63 ± 0.7	8.28 ± 0.5	7.67 ± 0.4	0.94 ± 0.1	57.53 ± 3.3

Abbreviations: NA, compounds having IC_{50} value > 50 μM; NT, not tested.

[a]IC_{50} values are the mean ± standard deviation of three separate experiments.

[b]0–10 μM: very strong; 10–20 μM: strong; 20–40 μM: moderate; 40–50 μM: weak.

Additionally, compounds **15_a**, **17**, and **19_d** showed weak activities against MCF-7 with IC_{50} values ranging from 43.47 to 48.33 μM, whereas compound **18_d** exhibited weak activities against HCT-116 and HepG-2 with IC_{50} values of 43.17 and 49.01 μM, respectively. Finally, compounds **14_a**, **14_b**, **15_c**, **16**, and **18_d** appeared to be inactive against MCF-7.

2.2.2 | Topoisomerase II inhibitory activity

As mentioned in the rationale of molecular design, we aimed to examine the inhibitory activity of the synthesized compounds against Topo II as a proposed mechanism of cytotoxic activity, such that the most cytotoxic compounds (**14_c**, **14_d**, **14_e**, **15_b**, **18_a**, **18_b**, **18_c**, **19_a**, and **19_b**) were further evaluated as Topo II inhibitors, based on the method described by Patra et al.[59] In this test, doxorubicin was utilized as a positive control. The IC_{50} values of the synthesized compounds against Topo II were determined from the concentration–inhibition response curve and summarized in Table 1.

The results revealed that some of the tested compounds potently inhibit Topo II activity, such as compounds **14_d** and **18_c** with IC_{50} values of 1.05 and 0.86 μM, respectively. These two compounds were 0.9 and 1.1 times as active as doxorubicin (IC_{50} = 0.94 μM). Additionally, some compounds exhibited moderate Topo II inhibitory activities such as compounds **14_c** (IC_{50} = 1.93 μM), **14_e** (IC_{50} = 1.78 μM), **18_a** (IC_{50} = 2.78 μM), and **18_b** (IC_{50} = 2.39 μM). On the contrary, compounds **15_b**, **19_a**, and **19_b** showed a weak Topo II inhibitory activity.

2.2.3 | DNA intercalation test

The compounds that exhibited higher cytotoxic activities were further evaluated for their DNA binding affinities. These compounds include **14_c**, **14_d**, **14_e**, **15_b**, **18_a**, **18_b**, **18_c**, **19_a**, and **19_b**. The DNA–methyl green assay was applied as described by Burre et al.[60] Doxorubicin, as an ideal DNA intercalator, was used as a positive control. The DNA binding affinity values were reported as IC_{50} values and summarized in Table 1.

TABLE 2 Apoptosis and necrosis percentage induced by compound **18$_c$** in HepG-2 cells

Sample	Apoptosis			Necrosis
	Total	Early	Late	
18$_c$/HepG-2	21.71	6.75	14.96	2.66
Cont. HepG-2	0.82	0.54	0.28	1.15

The tested compounds showed versatile DNA binding affinities. These affinities range from strong to weak. Compound **18$_c$** showed binding affinity higher than that of doxorubicin with an IC_{50} value of 48.53 μM. It was 1.16 times more active than doxorubicin. Additionally, compounds **14$_c$** and **14$_d$** showed comparable activities with doxorubicin with IC_{50} values of 59.13 and 54.52 μM, respectively. Moreover, compounds **14$_e$**, **15$_b$**, **18$_a$**, and **18$_b$** exhibited moderate DNA binding affinities with IC_{50} values ranging from 66.39 to 74.18 μM. On the contrary, compounds **19$_a$** and **19$_b$** showed weak binding activities with IC_{50} values of 82.04 and 79.63 μM, respectively.

2.2.4 | Apoptosis and cell-cycle analysis

Apoptosis initiation and cell cycle stages play an important role in cancer development. In cancer management, these two factors have a crucial role.[61,62] The most promising candidate **18$_c$** was selected to evaluate its impact on apoptosis and cell cycle profile. As HepG-2 cells were the most sensitive cells against the tested compounds, they were used for testing the apoptotic effect and cell cycle profile of compound **18$_c$**. Determination of apoptosis was carried out according to the reported annexin V and propidium iodide (PI) double-staining assay protocol.[63] In this test, HepG-2 cells were treated with compound **18$_c$** at a concentration that equals its IC_{50} value on HepG-2 (4.43 μM) for 24 h. The flow cytometry analysis was applied for the determination of apoptosis ratios of compound **18$_c$** in early- and late-stage apoptosis. The results are reported in Table 2 and Figure 2.

The results revealed that the two quadrant images describing damaged, necrotic/apoptotic, normal, and early apoptotic cells were detected in quadrants Q1, Q2, Q3, and Q4, respectively, during the flow cytometry analysis.[26] To calculate the apoptosis ratio, the values of both quadrants Q2 and Q4 were added. As shown in Figure 2, compound **18$_c$** has an apoptosis ratio of 21.71%, which is 12 times more than the control, 0.82%. These findings revealed that compound **18$_c$** can induce antiproliferative effect via induction of apoptosis.

The results of cell cycle analysis carried out in HepG-2 cells are presented in Table 3 and Figure 3. The results revealed that compound **18$_c$** produced 41.82% of cell accumulation in the G2–M phase. However, it produced only 18.24% of cell accumulation in G2–M in control (untreated cells). These results indicate that compound **18$_c$** induced a significant cell cycle arrest in the G2–M phase, compared with the control cells.

2.3 | Computational studies

2.3.1 | Molecular docking

Molecular docking studies were conducted for the synthesized compounds using doxorubicin as a reference standard. The main aim of this study was to gain further insights into the binding modes of the synthesized compounds against the Topo II–DNA complex (ID: 3qx3). Table 4 illustrates the binding free energies (ΔG) in negative values, reflecting the spontaneity of bindings. The reported binding site of DNA–Topo II complex consists of Asp479, Arg503, Gln778, Met782 Cyt8, Thy9, Cyt11, Gua13, and Ade12.[41]

The proposed doxorubicin binding mode showed an affinity value of −58.46 kcal/mol. A hydrogen bonding interaction was formed between the Cyt8 phosphate group and the NH_2 group of the sugar moiety. The OH group at position-12 was involved in hydrogen bonding interaction with Arg503. The aromatic planar system formed aromatic stacking interactions with various key residues as Thy9, Cyt8, Gua13, and Ade12. The side chain of sugar moiety was positioned in a minor groove of DNA (Figure 4).

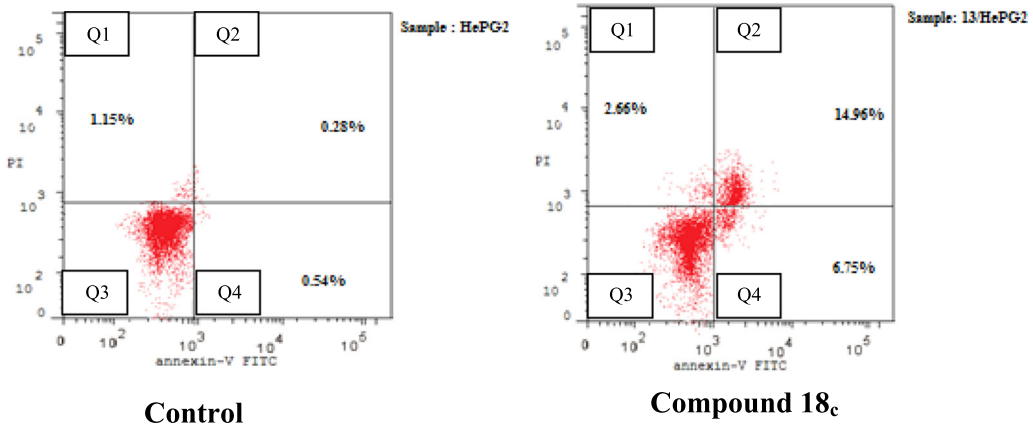

FIGURE 2 Induced apoptosis in HepG-2 cells by compound **18$_c$**

TABLE 3 Effect of compound 18_c on cell-cycle progression in HepG-2 cells

Sample	Cell cycle distribution (%)			
	G0–G1	S	G2–M	Pre-G1
18_c/HepG-2	30.25	27.93	41.82	24.37
Cont. HepG-2	50.47	31.29	18.24	1.97

The proposed binding mode of compound **13** showed an affinity value of −44.52 kcal/mol with three hydrogen bonds and eight $\pi-\pi$ interactions. The aromatic planar framework (1,2,4-triazolo[4,3-*c*]quinazoline) was involved in aromatic stacking interactions with DNA base pairs, Thy9, Cyt8, and Ade12. Furthermore, in the minor groove of DNA, the hydrazinyl group at position-5 was oriented and formed three hydrogen bonding interactions with the Thy9 phosphate group (Figure 5).

The proposed binding mode of compound 15_b showed an affinity value of −46.07 kcal/mol. It showed one hydrogen bonding interaction between the C═O of COOH group and Ade12. Additionally, the aromatic planar system (1,2,4-triazolo[4,3-*c*]quinazoline) exhibited aromatic interactions with Thy9 and Gua13. Moreover, the terminal benzoic acid moiety was oriented at the minor groove of DNA (Figure 6). The binding mode of compounds **16** and 18_b is illustrated in Supporting Information Data.

2.3.2 | In silico ADMET analysis

Discovery Studio 2.5 was used to predict ADMET descriptors (absorption, distribution, metabolism, excretion, and toxicity) for the designed compounds as compared with doxorubicin as a reference drug. Predicted ADMET studies for the tested compounds are illustrated in Table 5. It was found that BBB penetration of the designed compounds ranges from high to low, except compound 18_b, which was expected to be very low. This indicated that most compounds were anticipated to be safe for the CNS. Moreover, all the designed compounds were predicted to be absorbed better than doxorubicin. The enhancement of absorption was attributed to the polycyclic nucleus (1,2,4-triazolo[4,3-*c*]quinazoline), which increased the lipophilicity. Finally, the closer the hepatotoxicity scores to one, the more is the probability to be toxic, whereas the closer the hepatotoxicity scores to zero, the more is the probability to be nontoxic. Most of the designed compounds were predicted to be safer than doxorubicin, and the others were expected to be like doxorubicin. It is well known that numerous drug candidates have failed during clinical tests due to problems related to their absorption properties.[64] Upon computational investigation of the synthesized compounds, it was found that all the designed compounds have good absorption behavior. Moreover, the solubility level of most compounds was expected to be better than or even like that of the reference drug (Supporting Information Data).

2.4 | Structure–activity relationship (SAR)

As mentioned in the rationale of molecular design, we aimed at studying the SAR of the newly synthesized quinazoline derivatives as potential DNA intercalators and Topo II inhibitors. Observing the results of different biological tests, we could deduce significant data about SAR.

First, we investigated the effect of substitutions on position-5 of 1,2,4-triazolo[4,3-*c*]quinazoline nucleus by different amines. It was found that the substitutions with aliphatic amines (compounds 14_{c-e}) are more preferred biologically than that with aromatic amines (compounds 15_{a-c}). Concerning the activity of the different aliphatic amine derivatives, it was noted that alicyclic aliphatic amine (compound 14_d) is more active than that with open chain with the same length (compound 14_c). Moreover, the long-chain aliphatic amino derivative was more active than the corresponding members with a short aliphatic chain ($14_c > 14_b > 14_a$). Compound 15_b containing free carboxylic acid moiety was more active than the ester form 15_c.

Next, we studied the effect of substitutions at 5-position of 1,2,4-triazolo[4,3-*c*]quinazoline nucleus by different hydrazones and thiosemicarbazides. It was found that the hydrazones derivatives

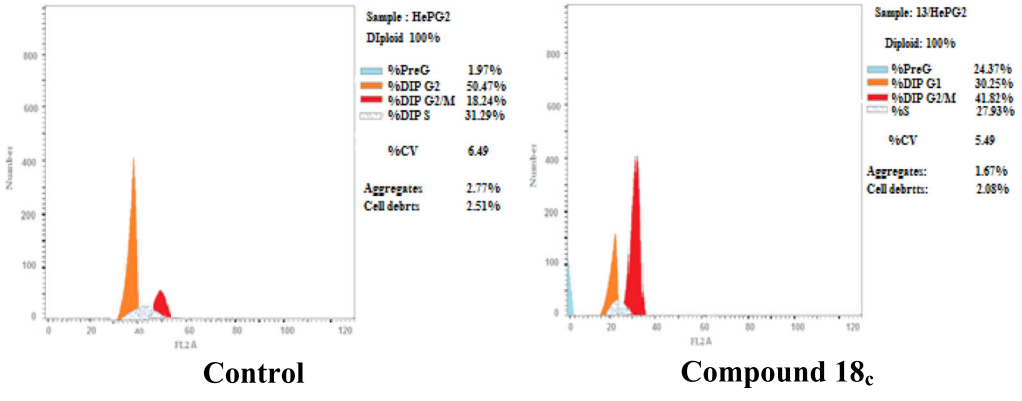

FIGURE 3 Distribution of HepG-2 cells upon treatment with compound 18_c

TABLE 4 The docking binding free energies of the synthesized compounds against DNA–Topo II complex forming hydrogen bonding and π–π interactions

Compound	ΔG kcal/mol	No. of H bonds	No. of π–π bonds	Putative interactions
13	−44.52	3	8	Ade12, Thy9, and Cyt8
14_a	−35.62	0	5	Ade12, Thy9, and Gua13
14_b	−39.24	0	7	Ade12, Thy9, and Gua13
14_c	−45.12	1	6	Ade12, Thy9, Gua13, and Arg503
14_d	−46.26	0	8	Ade12, Thy9, and Gua13
14_e	−43.15	0	7	Ade12, Thy9, and Cyt8
15_a	−41.29	0	9	Ade12, Thy9, and Gua13
15_b	−46.07	1	8	Ade12, Thy9, and Gua13
15_c	−40.26	0	8	Ade12, Thy9, and Gua13
16	−39.28	1	12	Ade12, Thy9, and Gua13
17	−36.90	0	5	Ade12, Thy9, and Cyt8
18_a	−44.68	1	4	Arg503, Thy9, Cyt8, and Gua13
18_b	−47.11	0	6	Gua13, Thy9, and Cyt8
18_c	−48.07	1	5	Asp479, Cyt8, Gua13, Ade12
18_d	−40.04	1	3	Arg503, Gln778, Thy9, Cyt8, and Ade12
19_a	−39.09	0	4	Gln778, Thy9, Cyt8, and Gua13
19_b	−41.15	0	6	Thy9, Cyt8, and Gua13
19_c	−42.67	1	5	Arg503, Cyt8, and Gua13
19_d	−40.16	1	3	Gln778, Gly504, Thy9, Cyt8, and Ade12
Doxorubicin	−58.46	2	6	Ade12, Thy9, Cyt8, Gua13, and Arg503

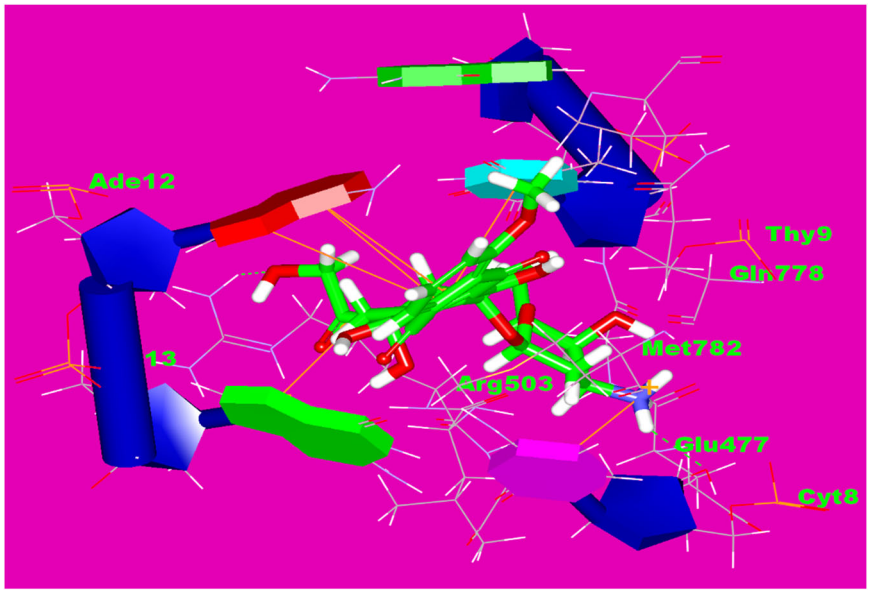

FIGURE 4 Doxorubicin in the active site of Topo II–DNA complex; hydrogen bonds are presented by green dashed lines and π–π interactions are presented by orange lines

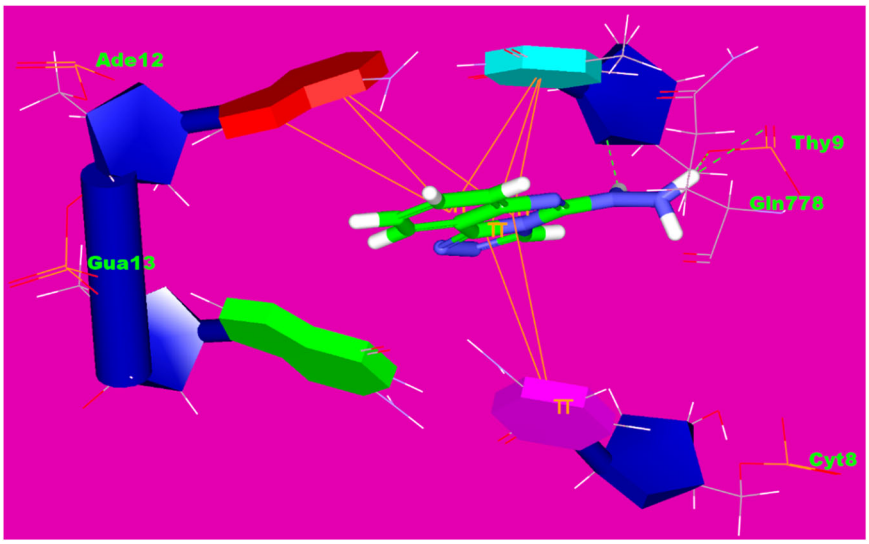

FIGURE 5 Compound **13** in the active site of Topo II–DNA complex; hydrogen bonds are presented by green dashed lines and π–π interactions are presented by orange lines

(compounds $\mathbf{18}_{a-c}$) are more active than thiosemicarbazides (compounds $\mathbf{19}_{a-d}$). Moreover, observing the activity of the substituted hydrazones, it was found that the derivatives with hydrophilic substitutions (compounds $\mathbf{18}_{b,c}$) were more active than the corresponding members with hydrophobic ones (compounds $\mathbf{18}_{a,d}$). Regarding the activity of different thiosemicarbazide derivatives, it was noted that aliphatic derivatives (compounds $\mathbf{19}_{a-c}$) were more active than aromatic one (compounds $\mathbf{19}_{d}$). Moreover, long-chain aliphatic thiosemicarbazide derivative was more active than the corresponding members with a short aliphatic chain ($\mathbf{19}_{c} > \mathbf{19}_{b} > \mathbf{19}_{a}$).

3 | CONCLUSION

In conclusion, a new series of 1,2,4-triazolo[4,3-*c*]quinazoline derivatives has been designed and synthesized. The synthesized compounds were evaluated for their in vitro cytotoxicity against three tumor cell lines (HCT-116, HepG-2, and MCF-7) by the MTT assay. Compounds $\mathbf{14}_{c}$, $\mathbf{14}_{d}$, $\mathbf{14}_{e}$, $\mathbf{15}_{b}$, $\mathbf{18}_{b}$, $\mathbf{18}_{c}$, and $\mathbf{19}_{b}$ exhibited promising antiproliferative activities. Compound $\mathbf{18}_{c}$ was the most cytotoxic member and exhibited superior antiproliferative activities against HCT-116 and HepG-2 with IC_{50} values of 5.22 and 4.43 μM, respectively, compared with doxorubicin (IC_{50} = 9.63 and 8.28 μM, respectively). Also, compound $\mathbf{14}_{d}$ showed higher activity than doxorubicin against HCT-116 cells (IC_{50} = 9.39 μM). In addition, compound $\mathbf{14}_{e}$ exhibited a higher activity than doxorubicin against HepG-2 with an IC_{50} value of 6.92 μM. The most promising antiproliferative members were assessed for their Topo II inhibitory activities and DNA intercalating affinities to deduce the proposed mechanism of antiproliferative effect. Some compounds displayed potent inhibitory activities against Topo II such as compounds $\mathbf{14}_{d}$ and $\mathbf{18}_{c}$ (IC_{50} = 1.05 and 0.86 μM, respectively). Moreover, the DNA intercalation assay revealed that compounds $\mathbf{14}_{d}$ and $\mathbf{18}_{c}$ (IC_{50} = 54.52 and 48.53 μM, respectively) were more active than doxorubicin (IC_{50} = 57.53 μM). Moreover, the flow cytometry analysis demonstrated that compound $\mathbf{18}_{c}$ could

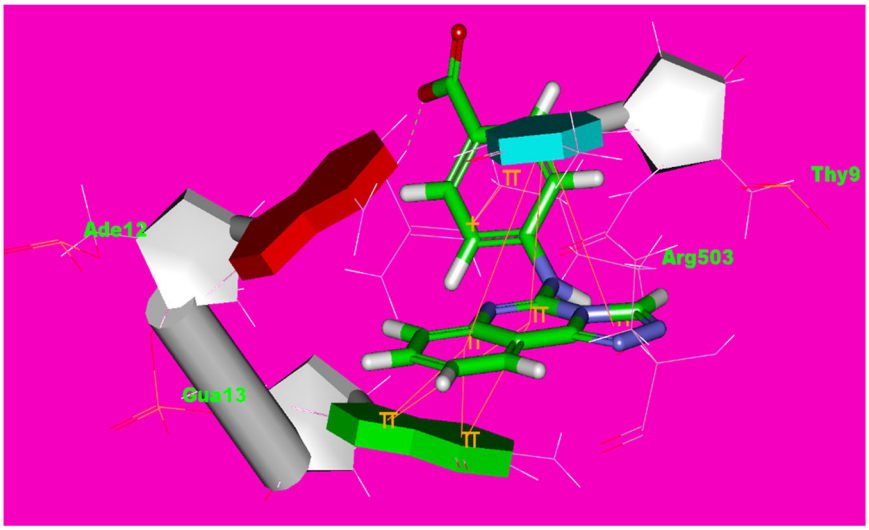

FIGURE 6 Compound $\mathbf{15}_{b}$ in the active site of Topo II–DNA complex; hydrogen bonds are presented by the green dashed lines and π–πinteractions are presented by orange lines

TABLE 5 Predicted ADMET (absorption, distribution, metabolism, excretion, and toxicity) descriptors for the designed compounds and doxorubicin

Compound No.	BBB level[a]	Absorption level[b]	Hepatotoxicity probability[c]	CYP2D6[d]	PPB[e]	Solubility level[f]
13	3	0	0.966	0	2	3
14_a	2	0	0.741	0	2	3
14_b	2	0	0.761	0	1	2
14_c	1	0	0.450	1	2	2
14_d	1	0	0.390	1	2	2
14_e	1	0	0.496	0	1	2
14_a	2	0	0.470	1	0	3
15_a	3	0	0.920	0	2	2
15_b	2	0	0.781	1	2	2
15_c	1	0	0.900	1	2	2
16	3	0	0.966	0	2	3
17	1	0	0.847	1	2	2
18_a	1	0	0.860	0	2	2
18_b	4	0	0.947	0	2	2
18_c	2	0	0.907	0	2	2
18_d	1	0	0.953	0	2	1
19_a	3	0	0.523	1	2	2
19_b	2	0	0.774	1	0	2
19_c	2	0	0.503	1	0	2
19_d	2	0	0.907	0	2	2
Doxorubicin	4	3	0.900	0	0	2

[a]BBB level, blood–brain barrier level, 0 = very high, 1 = high, 2 = medium, 3 = low, 4 = very low.
[b]Absorption level, 0 = good, 1 = moderate, 2 = poor, 3 = very poor.
[c]Hepatotoxicity probability, value > 0.5 means toxic, value < 0.5 means nontoxic.
[d]CYP2D6, cytochrome P2D6, 0 = noninhibitor, 1 = inhibitor.
[e]PBB, plasma protein binding, 0 means less than 90%, 1 means more than 90%, 2 means more than 95%.
[f]Solubility level, 0 = extremely low, 1 = very low, 2 = low, 3 = good, 4 = optimal.

significantly induce apoptosis (41.82%) in HepG-2 cells at a concentration of 4.43 μM and could arrest the cell cycle at the G2–M phase. In addition, the reported results allowed to draw an interesting SAR. In particular, The substitutions at 5-position of 1,2,4-triazolo[4,3-*c*]quinazoline nucleus by different aliphatic amines **14_{c-e}** were more preferred biologically than that with aromatic ones **15_{a-c}**. Moreover, alicyclic aliphatic amine **14_d** was more active than that with open chain with the same length **14_c**. Additionally, it was found that the derivatives with hydrazones substitutions **18_{a-c}** are more active than thiosemicarbazides **19_{a-d}**. Also, docking studies were carried out to explore the binding pattern of the designed compounds with the probable target, DNA–Topo II complex (PDB-code: 3qx3). Depending on the acquired results, we can conclude that DNA binding and/or Topo II inhibition may contribute to the detected cytotoxicity of the synthesized compounds.

4 | EXPERIMENTAL

4.1 | Chemistry

4.1.1 | General

All melting points were determined on a Gallenkamp apparatus using the open capillary method. The infrared spectra were reported using the potassium bromide disc technique on a Unicam SP 1000 IR spectrophotometer Pye. On a Jeol 400 MHz-NMR spectrometer, proton magnetic resonance ^{1}H NMR spectra are reported. Tetramethylsilane has been used as an internal norm, and chemical shifts have been calculated in the ppm range. The mass spectra were recorded on SHIMADZU GC/MS–QP5050A's Varian MAT 311-A (70 eV) and SHIMADZU GC/MS–QP5050A's Direct Inlet Unit (DI-50). All compounds in the theoretical values were within ± 0.4.

Thin-layer chromatography (TLC) monitored the reactions, using TLC sheets precoated with Merck 60 F254 UV fluorescent silica gel and visualized as mobile phases using UV lamps and various solvents. 5-Chloro-[1,2,4]triazolo[4,3-*c*]quinazoline **12** was obtained according to the reported procedures.[55]

The InChI codes of the investigated compounds, together with some biological activity data, are provided as Supporting Information.

4.1.2 | General procedure for the synthesis of 5-hydrazinyl-[1,2,4]triazolo[4,3-*c*]quinazoline (13)

A mixture of 5-chloro-[1,2,4]triazolo[4,3-*c*]quinazoline **12** (0.409 g, 0.002 mol) and hydrazine hydrate (0.128 g, 0.004 mol) was heated under reflux in isopropyl alcohol (IPA) (20 ml) for 1 h. After completion, the obtained crude solid was filtered and washed with IPA to give yellow solid of the desired compound **13**. Yellow powder (yield 85%); m.p. 227–229°C; IR (KBr, cm^{-1}); 3,302 (NH_2), 3,257 (NH), 3,051 (CH aromatic), and 1,637 (C═N); ^{1}H NMR (dimethyl sulfoxide [DMSO]-*d6*) δ ppm: 4.68 (s, 2H, NH_2), 7.38–7.42 (dd, J = 6.8 Hz, 1H, H-9 of quinazoline), 7.66–7.67 (d, J = 7.6 Hz, 1H, H-10 of quinazoline), 7.69–7.73 (dd, J = 6.8, 8 Hz, 1H, H-8 of quinazoline), 8.20–8.22 (d, J = 7.6 Hz, 1H, H-7 of quinazoline), 8.59 (s, 1H, CH triazole), and 9.30 (s, 1H, NH); MS (*m/z*): 200 (M^+, 15.40%), 167 (31.69%), 145 (59.89%), 97 (69.99%), 67 (52.69%), and 54 (100% base beak); Anal. calcd. for $C_9H_8N_6$ (200.21): C, 53.99; H, 4.03; N, 41.98; Found: C, 54.08; H, 4.01; N, 41.92%.

4.1.3 | General procedure for the synthesis of compounds 14_{a-e}

A mixture of compound **12** (0.409 g, 0.002 mol) and appropriate amines, namely ethylamine, *n*-propylamine, *n*-phenethylamine, cyclopentylamine, and diethylamine (0.004 mol), was refluxed in IPA (20 ml) for 2 h. After completion of the reaction, the crude solid was filtered and washed with IPA to give the corresponding target compounds $\mathbf{14_{a-e}}$, respectively.

N-*Ethyl-[1,2,4]triazolo[4,3-c]quinazolin-5-amine* (***14**$_a$*)

Gray crystal (yield, 72%); m.p. = 240–242°C. IR (KBr, cm^{-1}): 3,214 (NH), 3,046 (CH aromatic), 2,971 (CH aliphatic), and 1,635 (C═N); ^{1}H NMR (DMSO-*d*$_6$) δ ppm: 1.26–1.30 (t, 3H, CH_3), 3.54–3.61 (m, 2H, CH_2), 7.33–7.38 (dd, J = 7.6 Hz, 1H, H-9 of quinazoline), 7.52–7.54 (d, J = 7.6 Hz, 1H, H-10 of quinazoline), 7.58–7.62 (dd, J = 7.6 Hz, 1H, H-8 of quinazoline), 8.07–8.09 (t, 1H, NH), 8.22–8.24 (d, J = 7.6 Hz, 1H, H-7 of quinazoline), and 9.43 (s, 1H, CH triazole); Anal. calcd. for $C_{11}H_{11}N_5$ (213.24); C, 61.96; H, 5.20; N, 32.84. Found: C, 62.14; H, 5.12; N, 32.99%.

N-*Propyl-[1,2,4]triazolo[4,3-c]quinazolin-5-amine* (***14**$_b$*)

Shiny yellow crystal (yield, 80%); m.p. = 211–213°C. IR (KBr, cm^{-1}): 3,279 (NH), 3,057 (CH aromatic), 2,949 (CH aliphatic), and 1,630 (C═N); ^{1}H NMR (DMSO-*d*$_6$) δ ppm: 0.95–0.98 (t, 3H, CH_3), 1.65–1.74 (m, 2H, C**H**$_2$–CH_3), 3.46–3.51 (q, 2H, NH–C**H**$_2$), 7.30–7.34 (dd, J = 7.6 Hz, 1H, H-9 of quinazoline), 7.50–7.52 (d, J = 7.6 Hz, 1H, H-10 of quinazoline), 7.57–7.61 (dd, J = 7.6 Hz, 1H, H-8 of quinazoline), 8.05–8.07 (t, 1H, NH), 8.21–8.24 (d, J = 7.6 Hz, 1H, H-7 of quinazoline), and 9.45 (s, 1H, CH triazole); ^{13}C NMR (DMSO-*d*$_6$, 100 MHz) δ (ppm): 11.4, 21.7, 42.8, 112.1, 122.6, 123.4, 125.0, 131.5, 134.6, 141.2, 143.4, and 148.1; Anal. calcd. for $C_{12}H_{13}N_5$ (227.27); C, 63.42; H, 5.77; N, 30.82. Found: C, 63.73; H, 5.81; N, 30.78%.

N-*Pentyl-[1,2,4]triazolo[4,3-c]quinazolin-5-amine* (***14**$_c$*)

Shiny yellow crystal (yield, 69%); m.p. = 170–172°C. IR (KBr, cm^{-1}): 3,250 (NH), 3,087 (CH aromatic), 2,938 (CH aliphatic), and 1,632 (C═N); ^{1}H NMR (DMSO-*d*$_6$) δ ppm: 0.87–0.91 (t, 3H, CH_3), 1.33–1.41 (m, 4H, C**H**$_2$–C**H**$_2$–CH_3), 1.65–1.72 (p, 2H, NH-CH_2-C**H**$_2$), 3.51–3.56 (q, 2H, NH–C**H**$_2$), 7.32–7.36 (dd, J = 8.4 & 7.6 Hz, 1H, H-9 of quinazoline), 7.52–7.53 (d, J = 7.6 Hz, 1H, H-10 of quinazoline), 7.59–7.63 (dd, J = 8.4 Hz, 1H, H-8 of quinazoline), 8.05–8.08 (t, 1H, NH), 8.23–8.25 (d, J = 7.6 Hz, 1H, H-7 of quinazoline), and 9.48 (s, 1H, CH triazole); Anal. calcd. for $C_{14}H_{17}N_5$ (255.33); C, 65.86; H, 6.71; N, 27.43. Found: C, 65.98; H, 6.65; N, 27.54%.

N-*Cyclopentyl-[1,2,4]triazolo[4,3-c]quinazolin-5-amine* (***14**$_d$*)

Brown powder (yield, 78%); m.p. = 222–224°C. IR (KBr, cm^{-1}): 3,238 (NH), 3,051 (CH aromatic), 2,959 (CH aliphatic), and 1,630 (C═N); ^{1}H NMR (DMSO-*d*$_6$) δ ppm: 1.03–1.07 (m, 1H, H-3 of cyclopentyl), 1.54–1.68 (m, 3H, H-3 & H-4 of cyclopentyl), 1.74–1.76 (m, 2H, H-2 of cyclopentyl), 2.03–2.11 (m, 1H, H-5 of cyclopentyl), 3.42–3.46 (m, 1H, H-5 of cyclopentyl), 4.43–4.52 (m, 1H, H-1 of cyclopentyl), 7.31–7.35 (dd, J = 8 Hz, 1H, H-9 of quinazoline), 7.52–7.54 (d, J = 8 Hz, 1H, H-10 of quinazoline), 7.58–7.62 (dd, J = 8 Hz, 1H, H-8 of quinazoline), 7.82–7.84 (d, 1H, NH), 8.22–8.24 (d, J = 8 Hz, 1H, H-7 of quinazoline), and 9.55 (s, 1H, CH triazole); Anal. calcd. for $C_{14}H_{15}N_5$ (253.31); C, 66.38; H, 5.97; N, 27.65. Found: C, 66.59; H, 6.11; N, 27.78%.

N,N-*Diethyl-[1,2,4]triazolo[4,3-c]quinazolin-5-amine* (***14**$_e$*)

Yellowish brown (yield, 76%); m.p. = 180–182°C. IR (KBr, cm^{-1}): 3,124 (NH), 3,072 (CH aromatic), 2,961 (CH aliphatic), and 1,609 (C═N); ^{1}H NMR (DMSO-*d*$_6$) δ ppm: 1.23–1.27 (t, 6H, $2CH_3$), 3.59–3.64 (q, 4H, $2CH_2$), 7.44–7.48 (dd, J = 8 Hz, 1H, H-9 of quinazoline), 7.60–7.62 (d, J = 8 Hz, 1H, H-10 of quinazoline), 7.65–7.69 (dd, J = 8 & 7.6 Hz, 1H, H-8 of quinazoline), 8.30–8.32 (d, J = 7.6 Hz, 1H, H-7 of quinazoline), and 9.23 (s, 1H, CH triazole); Anal. calcd. for $C_{13}H_{15}N_5$ (241.30); C, 64.71; H, 6.27; N, 29.02. Found: C, 64.87; H, 6.30; N, 29,11%.

4.1.4 | General procedure for the synthesis of compounds 15_{a-c}

A mixture of 5-chloro-[1,2,4]triazolo[4,3-*c*]quinazoline **12** (0.409 g, 0.002 mol) and the appropriate aromatic amines, namely 4-methylaniline,

4-aminobenzoic acid, and ethyl *p*-aminobenzoate (0.006 mol), in IPA (20 ml) was refluxed for 7 h. After completion, the obtained precipitate was filtered and washed with IPA to give the corresponding title compounds **15$_{a–c}$**, respectively.

*N-(p-Tolyl)-[1,2,4]triazolo[4,3-c]quinazolin-5-amine (**15$_a$**)*

Yellowish white powder (yield, 83%); m.p. = 214–216°C; IR (KBr, cm^{-1}): 3,137 (NH), 3,065 (CH, aromatic), and 1,629 (C═N); ^{1}H NMR (DMSO-d_6) δ ppm: 2.32 (s, 3H, CH_3), 7.21–7.23 (d, J = 8 Hz, 2H, H-2 and H-6 phenyl), 7.42–7.45 (dd, J = 7.6 Hz, 1H, H-9 of quinazoline), 7.58–7.60 (d, J = 8 Hz, 1H, H-10 of quinazoline), 7.64–7.68 (dd, J = 8 Hz, 1H, H-8 of quinazoline), 7.90–7.92 (d, J = 8 Hz, 2H, H-3 and H-5 phenyl), 8.29–8.31 (d, J = 8 Hz, 1H, H-7 of quinazoline), 10.30 (s, 1H, CH triazole), and 10.44 (s, 1H, NH); Anal. calcd. for $C_{16}H_{13}N_5$ (275.32); C, 69.80; H, 4.76; N, 25.44. Found: C, 69.91; H, 4.81; N, 25.49%.

*4-([1,2,4]Triazolo[4,3-c]quinazolin-5-ylamino)benzoic acid (**15$_b$**)*

Shiny yellow powder (yield, 78%); m.p. = 225–227°C; IR (KBr, cm^{-1}): 3,175 (NH), 3,046 (CH, aromatic), and 1,674 (C═N); ^{1}H NMR (DMSO-d_6) δ ppm: 7.51–7.57 (dd, J = 7.6 Hz, 1H, H-9 of quinazoline), 7.72–7.83 (d, J = 8 Hz, 2H, H-2 and H-6 phenyl), 7.98–8.02 (d, J = 8 Hz, 2H, H-3 and H-5 phenyl), 8.11–8.13 (d, J = 8 Hz, 1H, H-10 of quinazoline), 8.27–8.30 (dd, J = 8 Hz, 1H, H-8 of quinazoline), 8.35–8.37 (dd, J = 7.6 Hz, 1H, H-7 of quinazoline), 9.38 (s, 1H, CH triazole), 10.42 (s, 1H, NH), and 12.35 (s, 1H, OH); Anal. calcd. for $C_{16}H_{11}N_5O_2$ (305.30); C, 62.95; H, 3.63; N, 22.94. Found: C, 63.08; H, 3.71; N, 22.91%.

*Ethyl 4-([1,2,4]triazolo[4,3-c]quinazolin-5-ylamino)benzoate (**15$_c$**)*

Shiny yellow powder (yield, 81%); m.p. = 169–171°C; IR (KBr, cm^{-1}): 3,189 (NH), 3,055 (CH, aromatic), 1,704 (C═O), and 1,643 (C═N); ^{1}H NMR (DMSO-d_6) δ ppm: 1.32–136 (t, 3H, CH_3), 4.29–4.34 (q, 2H, CH_2), 7.49–7.53 (dd, J = 8 Hz, 1H, H-9 of quinazoline), 7.70–7.75 (m, 2H, H-8 of quinazoline and H-10 of quinazoline), 8.01–8.04 (d, J = 8 Hz, 2H, H-2 and H-6 phenyl), 8.13–8.15 (d, J = 8 Hz, 2H, H-3 and H-5 phenyl), 8.34–8.36 (d, J = 8 Hz, 1H, H-7 of quinazoline), 9.93 (s, 1H, CH triazole), and 10.40 (s, 1H, NH); ^{13}C NMR (DMSO-d_6, 100 MHz) δ (ppm): 14.0, 60.2, 112.8, 119.9 (2C), 122.6, 124.1, 125.2, 125.4, 129.8 (2C), 131.7, 135.4, 137.5, 141.7, 143.1, 147.8, and 165.1; Anal. calcd. for $C_{18}H_{15}N_5O_2$ (333.35); C, 64.86; H, 4.54; N, 21.01. Found: C, 64.96; H, 4.58; N, 21.11%.

4.1.5 | General procedure for the synthesis of *N*-benzyl-[1,2,4]triazolo[4,3-*c*]quinazolin-5-amine (16)

A mixture of 5-chloro-[1,2,4]triazolo[4,3-*c*]quinazoline **12** (0.409 g, 0.002 mol) and benzylamine (0.428 g, 0.004 mol) in IPA (20 ml) was refluxed for 1 h. After completion, the obtained crude solid was filtered and washed with IPA to give yellow solid of the desired compound **16**. Yellow powder (yield, 89%); m.p. = 216–218°C; IR (KBr, cm^{-1}): 3,279 (NH), 3,066 (CH, aromatic), 2,925 (CH aliphatic), and 1,628 (C═N); ^{1}H NMR (DMSO-d_6) δ ppm: 4.78–4.79 (d, 2H, CH_2), 7.23–7.27 (dd, J = 7.6 Hz, 1H, H-9 of quinazoline), 7.31–7.36 (m, J = 7.6 Hz, 3H, H-3, H-4 and H-5 phenyl), 7.44–7.46 (d, J = 7.6 Hz, 2H, H-2 and H-6 phenyl), 7.50–7.52 (d, J = 8 Hz, 1H, H-10 of quinazoline), 7.58–7.62 (dd, J = 8 Hz, 1H, H-8 of quinazoline), 8.23–8.25 (d, J = 7.6 Hz, 1H, H-7 of quinazoline), 8.68 (s, 1H, NH), and 9.49 (s, 1H, CH triazole); ^{13}C NMR (DMSO-d_6, 100 MHz) δ (ppm): 44.2, 112.3, 122.7, 123.7, 125.1, 127.1, 127.6 (2C), 128.3 (2C), 131.5, 134.7, 138.5, 141.3, 143.3, and 148.1; Anal. calcd. for $C_{16}H_{13}N_5$ (275.32); C, 69.80; H, 4.76; N, 25.44. Found: C, 69.91; H, 4.81; N, 25.49%.

4.1.6 | General procedure for the synthesis of 4-([1,2,4]triazolo[4,3-*c*]quinazolin-5-yl)morpholine (17)

A mixture of 5-chloro-[1,2,4]triazolo[4,3-*c*]quinazoline **12** (0.409 g, 0.002 mol) and morpholine (0.348 g, 0.004 mol) in IPA (20 ml) was refluxed for 3 h. After completion, the obtained crude solid was filtered and washed with IPA to give the desired compound **17**. White powder (yield, 88%); m.p. = 210–212°C. IR (KBr, cm^{-1}): 3,117 (NH), 2,975 (CH aliphatic), and 1,617 (C═N); ^{1}H NMR (DMSO-d_6) δ ppm: 3.50–3.52 (t, 4H, 2CH_2–O), 3.82–3.83 (t, 4H, 2CH_2–N), 7.53–7.57 (dd, J = 8 Hz, 1H, H-9 of quinazoline), 7.71–7.73 (d, J = 7.6 Hz, 2H, H-8 and H-10 of quinazoline), 8.35–8.37 (d, J = 7.6 Hz, 1H, H-7 of quinazoline), and 9.49 (s, 1H, CH triazole); ^{13}C NMR (DMSO-d_6, 100 MHz) δ (ppm): 49.3 (2C), 66.0 (2C), 114.4, 123.1, 126.6, 126.7, 132.1, 136.7, 142.1, 144.7, and 149.2; Anal. calcd. for $C_{13}H_{13}N_5O$ (255.28); C, 61.17; H, 5.13; N, 27.43. Found: C, 61.26; H, 5.19; N, 27.52%.

4.1.7 | General procedure for the synthesis of compounds 18$_{a–d}$

A mixture of 5-hydrazinyl-[1,2,4]triazolo[4,3-*c*]quinazoline **13** (0.400 g, 0.002 mol) and the appropriate aldehydes, namely 4-methylbenzaldhehyde, 4-nitrobenzaldhehyde, 4-hydroxybenzaldhehyde, and 2,6-dichlorobenzaldhehyde (0.0024 mol), was refluxed in absolute ethanol (25 ml) in the presence of catalytic amount of glacial acetic acid for 6 h. The mixture was cooled, filtered, and crystallized from ethanol to afford the corresponding derivatives **18$_{a–d}$**, respectively.

*(E)-5-[2-(4-Methylbenzylidene)hydrazinyl]-[1,2,4]triazolo[4,3-c]-quinazoline (**18$_a$**)*

Canary yellow powder (yield, 76%); m.p. = 220–222°C; IR (KBr, cm^{-1}): 3,131 (NH), 3,044 (CH, aromatic), and 1,627 (C═N); ^{1}H NMR (DMSO-d_6) δ ppm: 2.31 (s, 3H, CH_3), 7.20–7.22 (d, J = 8 Hz, 2H, H-3 and H-5 phenyl), 7.41–7.45 (dd, J = 7.6 Hz, 1H, H-9 of quinazoline), 7.58–7.60 (d, J = 8 Hz, 1H, H-10 of quinazoline), 7.64–7.68 (dd, J = 8 Hz, 1H, H-8 of quinazoline), 7.91–7.93 (d, J = 8 Hz, 2H, H-2 and H-6 phenyl), 8.29–8.31 (d, J = 8 Hz, 1H, H-7 of quinazoline), 8.71 (s, 1H, N═CH), 10,36 (s, 1H, CH triazole), and 10.50 (s, 1H, NH); ^{13}C NMR (DMSO-d_6, 100 MHz) δ (ppm): 20.5, 113.0, 121.5 (2C), 122.7,

124.5, 125.5 (2C), 128.9 (2C), 131.6, 132.6, 135.9, 136.0, 138.7, 142.6, 148.1; Anal. calcd. for $C_{17}H_{14}N_6$ (302.34); C, 67.54; H, 4.67; N, 27.80. Found: C, 67.61; H, 4.74; N, 27.86%.

*(E)-5-[2-(4-Nitrobenzylidene)hydrazinyl]-[1,2,4]triazolo[4,3-c]-quinazoline (**18**$_b$)*

Yellow powder (yield, 78%); m.p. = 230–232°C; IR (KBr, cm^{-1}): 3,318 (NH), 3,089 (CH, aromatic), and 1,642 (C=N); ^{1}H NMR (DMSO-d_6) δ ppm: 7.33–7.35 (dd, 1H, H-9 of quinazoline), 7.82–7.84 (d, J = 8 Hz, 2H, H-2 and H-6 phenyl), 8.01–8.03 (d, 1H, H-10 of quinazoline), 8.11–8.13 (dd, 1H, H-8 of quinazoline), 8.30–8.32 (d, J = 8 Hz, 2H, H-3 and H-5 phenyl), 8.34 (s, 1H, N=CH), 8.53–8.55 (d, 1H, H-7 of quinazoline), 8.70 (s, 1H, CH triazole), and 11.53 (s, 1H, NH); Anal. calcd. for $C_{16}H_{11}N_7O_2$ (333.31); C, 57.66; H, 3.33; N, 29.42. Found: C, 57.71; H, 3.35; N, 29.38%.

*(E)-4-{[2-([1,2,4]Triazolo[4,3-c]quinazolin-5-yl)hydrazono]methyl}-phenol (**18**$_c$)*

Gray powder (yield, 71%); m.p. = 215–217°C; IR (KBr, cm^{-1}): 3,141 (NH), 3,048 (CH, aromatic), and 1,652 (C=N); ^{1}H NMR (DMSO-d_6) δ ppm: 6.85–6.88 (d, J = 7.6 Hz, 2H, H-3 and H-5 phenyl), 7.34–7.37 (dd, J = 7.6 Hz, 1H, H-9 of quinazoline), 7.67–7.70 (d, J = 8 Hz, 1H, H-10 of quinazoline), 7.75–7.81 (m, 3H, H-8 of quinazoline, H-2 and H-6 phenyl), 8.15–8.17 (d, J = 7.6 Hz, 1H, H-7 of quinazoline), 8.51 (s, 1H, N=CH), 8.57 (s, 1H, CH triazole), 9.25 (s, 1H, OH), and 9.80 (s, 1H, NH); ^{13}C NMR (DMSO-d_6, 100 MHz) δ (ppm): 116.09 (2C), 116.28, 123.65, 124.04, 125.47, 126.12, 130.02, 130.58, 132,91, 151.21, 154.01, 160.11 (2C), 160.86, and 160.93; MS (*m/z*): 304 (M^+, 2.33%), 240 (13.31%), 185 (25.25%), 147 (15.13%), 120 (22.24%), 105 (31.07%), 77 (84.29%), 65 (100% base beak), and 64 (39.69%); Anal. calcd. for $C_{16}H_{12}N_6O$ (304.31); C, 63.15; H, 3.97; N, 27.62. Found: C, 63.21; H, 4.04; N, 27.54%.

*(E)-5-[2-(2,6-Dichlorobenzylidene)hydrazinyl]-[1,2,4]triazolo[4,3-c]-quinazoline (**18**$_d$)*

Yellowish white powder (yield, 79%); m.p. = 254–256°C; IR (KBr, cm^{-1}): 3,148 (NH), 3,092 (CH, aromatic), and 1,645 (C=N); ^{1}H NMR (DMSO-d_6) δ ppm: 7.27–7.31 (dd, J = 7.6 Hz, 1H, H-9 of quinazoline), 7.46–7.50 (dd, J = 8 Hz, 1H, H-8 of quinazoline), 7.55–7.61 (m, J = 8 Hz, 3H, H-3, H-4 and H-5 phenyl), 7.74–7.76 (d, 1H, H-10 of quinazoline), 8.14–8.16 (d, J = 8 Hz, 1H, H-7 of quinazoline), 8.61 (s, 1H, N=CH), 9.33 (s, 1H, CH triazole), and 11.28 (s, 1H, NH); ^{13}C NMR (DMSO-d_6, 100 MHz) δ (ppm): 109.4, 116.5, 123.1, 123.2, 128.7 (2C), 131.3, 131.7, 132.0, 134.2 (2C), 135.4, 137.5, 143.7, 146.5, and 151.4; Anal. calcd. for $C_{16}H_{10}Cl_2N_6$ (356.03); C, 53.80; H, 2.82; N, 23.53. Found: C, 53.92; H, 2.85; N, 23.56%.

4.1.8 | General procedure for the synthesis of compounds 19$_{a–d}$

A mixture of 5-hydrazinyl-[1,2,4]triazolo[4,3-c]quinazoline **13** (0.409 g, 0.002 mol) and the appropriate isothiocyanates, namely ethyl isothiocyanate, propyl isothiocyanate, butyl isothiocyanate, and phenyl isothiocyanate (0.003 mol), was refluxed in ethanol (25 ml) for 3 h. The reaction mixture was cooled, and the separated solids were filtered and crystallized from ethanol to afford the corresponding compounds **19**$_{a–d}$, respectively.

*2-([1,2,4]Triazolo[4,3-c]quinazolin-5-yl)-N-ethylhydrazine-1-carbothioamide (**19**$_a$)*

Shiny yellow powder (yield, 74%); m.p. = 243–245°C; IR (KBr, cm^{-1}): 3,205 (NH), 2,969 (CH, aliphatic), and 1,637 (C=N); ^{1}H NMR (DMSO-d_6) δ ppm: 1.04–1.06 (t, 3H, CH_3), 3.45–3.48 (q, 2H, CH_2), 7.48–7.52 (dd, J = 7.2 Hz, 1H, H-9 of quinazoline), 7.71–7.75 (m, 2H, H-8 of quinazoline and H-10 of quinazoline), 8.24 (s, 1H, N**H**–CH_2), 8.28–8.30 (d, J = 7.2 Hz, 1H, H-7 of quinazoline), 8.68 (s, 1H, CH triazole), 9.57 (s, 1H, N**H**-quinazoline), and 10.20 (s, 1H, N**H**–C=S); ^{13}C NMR (DMSO-d_6, 100 MHz) δ (ppm): 14.4, 38.5, 114.2, 123.2, 124.5, 125.8, 132.3, 143.1, 143.8, 151.0, 153.4, and 181.3; Anal. calcd. for $C_{12}H_{13}N_7S$ (287.35); C, 50.16; H, 4.56; N, 34.12. Found: C, 50.24; H, 4.61; N, 34.18%.

2-([1,2,4]Triazolo[4,3-c]quinazolin-5-yl)-N-propylhydrazine-1-carbothioamide (19$_b$)

Gray powder (yield, 77%); m.p. = 229–231°C; IR (KBr, cm^{-1}): 3,173 (NH), 2,954 (CH, aliphatic), and 1,626 (C=N); ^{1}H NMR (DMSO-d_6) δ ppm: 0.78–0.82 (t, 3H, CH_3), 1.73–1.82 (m, 2H, C**H**$_2$–CH_3), 4.03–4.07 (t, 2H, NH–C**H**$_2$), 7.08–7.11 (dd, J = 7.6 Hz, 1H, H-9 of quinazoline), 7.45–7.47 (d, 1H, H-10 of quinazoline), 7.70–7.74 (dd, 1H, H-8 of quinazoline), 8.24–8.26 (m, 2H, N**H**–CH_2 and H-7 of quinazoline), 8.67 (s, 1H, CH triazole), 9.55 (s, 1H, N**H**-quinazoline), and 10.21 (s, 1H, N**H**–C=S); Anal. calcd for $C_{13}H_{15}N_7S$ (301.37); C, 51.81; H, 5.02; N, 32.53. Found: C, 51.98; H, 4.94; N, 32.61%.

*2-([1,2,4]Triazolo[4,3-c]quinazolin-5-yl)-N-butylhydrazine-1-carbothioamide (**19**$_c$)*

White powder (yield, 79%); m.p. = 199–201°C; IR (KBr, cm^{-1}): 3,203 (NH), 2,936 (CH, aliphatic), and 1,637 (C=N); ^{1}H NMR (DMSO-d_6) δ ppm: 0.80–0.83 (t, 3H, CH_3), 1.22–1.24 (m, 2H, C**H**$_2$–CH_3), 1.44–1.47 (m, 2H, C**H**$_2$–CH_2–CH_3), 4.42–3.44 (t, 2H, NH–C**H**$_2$), 7.47–7.51 (dd, J = 7.6 Hz, 1H, H-9 of quinazoline), 7.68–7.70 (d, J = 7.6 Hz, 1H, H-10 of quinazoline), 7.73–7.77 (dd, J = 7.6 Hz, 1H, H-8 of quinazoline), 8.70 (s, 1H, NH-CH_2), 8.27-8.29 (d, J = 7.6 Hz, 1H, H-7 of quinazoline), 8.67 (s, 1H, CH triazole), 9.53 (s, 1H, NH-quinazoline), and 10.19 (s, 1H, NH–C=S); Anal. calcd. for $C_{14}H_{17}N_7S$ (315.40); C, 53.31; H, 5.43; N, 31.09. Found: C, 53.44; H, 5.47; N, 31.21%.

*2-([1,2,4]Triazolo[4,3-c]quinazolin-5-yl)-N-phenylhydrazine-1-carbothioamide (**19**$_d$)*

Pale yellow powder (yield, 70%); m.p. = 182–185°C; IR (KBr, cm^{-1}): 3,199 (NH), 3,062 (CH, aromatic), and 1,607 (C=N); ^{1}H NMR (DMSO-d_6) δ ppm: 7.12–7.16 (t, J = 7.6 Hz, 1H, H-5 phenyl), 7.31–7.35 (dd, J = 8 Hz, 1H, H-9 of quinazoline), 7.50–7.54 (m, 3H, H-3, H-5 phenyl and H-10 of quinazoline), 7.65–7.68 (m, 3H, H-2, H-6 phenyl and H-8 of quinazoline), 8.04 (s, 1H, N**H**-quinazoline),

8.28–8.30 (d, 1H, H-7 of quinazoline), 9.66 (s, 1H, CH triazole), 11.07 (s, 1H, N**H**–C=S), and 13.41 (s, 1H, N**H**-phenyl); ^{13}C NMR (DMSO-d_6, 100 MHz) δ (ppm): 117.5, 121.2, 125.0, 127.4, 128.3, 129.5 (2C), 130.0 (2C), 130.3, 132.3, 137.4, 139.3, 143.0, 148.3, and 164.9; Anal. calcd. for $C_{16}H_{13}N_7S$ (335.39); C, 57.30; H, 3.91; N, 29.23. Found: C, 57.44; H, 3.97; N, 29.36%.

4.2 | Biological testing

4.2.1 | In vitro antiproliferative activities

The synthesized compounds were evaluated for their antiproliferative activities against three human cancer cell lines, namely colorectal carcinoma (HCT-116), hepatocellular carcinoma (HepG-2), and breast cancer (MCF-7). The MTT assay protocol was applied as described.[56–58]

Cell lines were cultured in the RPMI-1640 medium with 10% fetal bovine serum. Antibiotics, 100 units/ml penicillin and 100 µg/ml streptomycin, were added at 37°C in a 5% CO_2 incubator. The cell lines were seeded in a 96-well plate at a density of 1.0×10^4 cells/well at 37°C for 48 h under 5% CO_2. After incubation, the cells were treated with different concentration of the synthesized compounds and incubated for 24 h. Then, 20 µl of the MTT solution at a concentration of 5 mg/ml was added and incubated for 4 h. DMSO in volume of 100 µl was added into each well to dissolve the purple formazan formed. The colorimetric assay was measured and recorded at an absorbance of 570 nm using a plate reader (EXL 800). The relative cell viability in percentage was calculated as (A570 of treated samples/A570 of untreated sample) × 100. Results for IC_{50} values of the active compounds are summarized in Table 1.

4.2.2 | Measurement of topoisomerase II activity

Nine compounds that showed high antiproliferative activities (**14_c**, **14_d**, **14_e**, **15_b**, **18_a**, **18_b**, **18_c**, **19_a**, and **19_b**) were further assessed to determine their inhibitory activities against Topo II. Topo II drug screening kit (TopoGEN, Inc.) was used to determine the activity of Topo II according to a previously reported procedure by Patra et al.[65] Doxorubicin as a potent Topo II inhibitor was used as positive control in this test.

In general, the reaction was allowed to start by incubating a mixture of human Topo II (2 µl), substrate supercoiled pHot1 DNA (0.25 µg), 50 µg/ml test compound (2 µl), and assay buffer (4 µl) in 37°C for 30 min. To terminate the reaction, 10% sodium dodecylsulphate (2 µl) and proteinase K (50 µg/ml) were added at 37°C for 15 min, followed by incubation for 15 min at 37°C. Then, the DNA was run on 1% agarose gel in BioRad gel electrophoresis system for 1–2 h, followed by staining with GelRed™ stain for 2 h and destaining for 15 min with TAE buffer (Tris base, acetic acid, and EDTA). The gel was imaged via BioRad's Gel DocTMEZ system. Both supercoiled and linear strands DNA were incorporated in the gel as markers for DNA–Topo II intercalators. The results were reported as IC_{50} (50% inhibition concentration) values calculated from the concentration–inhibition response curve.

4.2.3 | DNA intercalation assay

Nine compounds that exhibited significant antiproliferative activities (**14_c**, **14_d**, **14_e**, **15_b**, **18_a**, **18_b**, **18_c**, **19_a**, and **19_b**) were further evaluated to determine their DNA-binding affinities. Doxorubicin as a DNA intercalator was used as a positive control. In this test, methyl green dye can bind with DNA to form a colored reversible complex of DNA/methyl green. These complexes stay stable at neutral pH. Upon addition of intercalating agents, the methyl green is displaced from DNA with the addition of H_2O molecule to the dye, resulting in the formation of the colorless carbinol, leading to a dramatic decrease in spectrophotometric absorbance.[60] The difference between DNA/methyl green complex and free cabinol provides the simplest means for detecting the DNA-binding affinity and relative binding strength. IC_{50} values were determined using the GraphPad Prism 5.0 software. The reaction was performed as follows. Calf thymus DNA (10 mg) and methyl green (20 mg) (Sigma-Aldrich) were added in 100 ml of 0.05 M Tris-HCl buffer (pH 7.5) containing 7.5 mM $MgSO_4$. Then, the mixture was stirred for 24 h at 37°C. The test samples were dissolved in ethanol and dispensed into wells of a 96-well microtiter tray at concentrations of 10, 100, and 1,000 µM. From each well, the excess solvent was removed under vacuum, followed by an addition of 200 µl of the DNA/methyl green solution. The test samples were incubated in the dark at an ambient temperature. After 24 h, the absorbance of each sample was determined at 642.5–645 nm. Readings were corrected for initial absorbance and normalized as the percentage of the untreated DNA/methyl green absorbance value.

4.2.4 | Flow cytometric analysis of the cell cycle

According to the method described by Léonce et al.,[66] the flow cytometric analysis was carried out. In this test, PI is used to discriminate between living cells from dead ones or for cell cycle analysis. The cell cycle analysis is based on the stoichiometric binding of PI to intracellular DNA. HepG-2 cells were seeded in 100-mm culture dishes and immediately incubated with the test compound **18_c**. After 24 h, the cells were washed, fixed, and stained in phosphate-buffered saline (PBS), Triton X-100 (0.1%), RNase A (1 mg/ml), and 0.5 ml of PI in PBS (1 mg/ml). Then, the DNA content was determined with a flow cytometer and the distribution of cells in pre-G1 (apoptotic cells), G0–G1, S, and G2–M peaks was quantified by the histogram analysis. The obtained data represent three independent experiments.

4.2.5 | Apoptosis using annexin-V-FITC assay

Annexin V-fluorescein isothiocyanate (FITC)/PI apoptosis detection kit was used in staining HepG-2 cells, which were stained with

annexin V-FITC and counterstained with PI. Cells were incubated with the tested compound **18$_c$** for 24 h and 48 h. Then, they were trypsinized and washed with cold PBS two times, and then stained with 5 µl annexin V-FITC in a binding buffer (10 mM HEPES, 140 mM NaCl, and 2.5 mM $CaCl_2$ at pH 7.4) for 15 min at room temperature in the dark. The samples were analyzed using the flow cytometer.[63]

4.3 | In silico studies

4.3.1 | Molecular docking

The title molecules were investigated with the aid of docking studies using Discovery Studio 2.5 for their binding capabilities for DNA–Topo II. The three-dimensional (3D) crystal structure of DNA–Topo II was recovered from the Protein Data Bank (PDB ID: 3qx3, resolution: 2.16 Å). First, molecules of water were removed from the complex. Using the valence monitor method, the incorrect valence atoms were corrected. The energy minimization was then accomplished through the application of force fields CHARMM and MMFF94. The binding site of the complex was defined and prepared for docking. Structures of the synthesized compounds and doxorubicin were sketched using ChemBioDraw Ultra 14.0 and saved in MDL-SD file format. Next, the MDL-SD file was opened, 3D structures were protonated, and energy was minimized by implementing force fields CHARMM and MMFF94, and then adjusted for docking. CDOCKER protocol was used for docking studies using CHARMM-based molecular dynamics to dock ligands into a receptor binding site. In the docking studies, a total of 10 conformers were considered for each molecule. Finally, according to the minimum free energy of the DNA–Topo II ligand interactions, the most ideal pose was chosen.

4.3.2 | In silico ADMET analysis

ADMET descriptors (absorption, distribution, metabolism, excretion, and toxicity) of the compounds were determined using Discovery Studio 2.5. First, the CHARMM force field was applied, then the tested compounds were prepared, and the energy was minimized according to the preparation of small molecule protocol. Next, ADMET descriptors protocol was applied to calculate the different descriptors.

CONFLICTS OF INTERESTS

The authors declare that there are no conflicts of interests.

ORCID

Mohamed S. Alesawy https://orcid.org/0000-0001-9202-1754
Ahmed A. Al-Karmalawy https://orcid.org/0000-0002-8173-6073
Eslam B. Elkaeed https://orcid.org/0000-0002-2546-8035
Ahmed Belal https://orcid.org/0000-0002-9913-5380
Ibrahim H. Eissa https://orcid.org/0000-0002-6955-2263

REFERENCES

[1] A. Jemal, T. Murray, E. Ward, A. Samuels, R. C. Tiwari, A. Ghafoor, E. J. Feuer, M. J. Thun, *CA Cancer J. Clin.* **2005**, *55*(*1*), 10.
[2] I. J. Fidler, *Cancer Res.* **1985**, *45*(*10*), 4714.
[3] WHO, Cancer, Key facts, https://www.who.int/news-room/fact-sheets/detail/cancer (accessed: October 2019).
[4] R. L. Siegel, K. D. Miller, A. Jemal, *CA Cancer J. Clin.* **2016**, *66*(*1*), 7.
[5] L. H. Hurley, *Nat. Rev. Cancer* **2002**, *2*(*3*), 188.
[6] C. Avendano, J. C. Menendez, *Medicinal Chemistry of Anticancer Drugs*, *Chapter 7* **2008**, p. 200.
[7] R. Ducray, P. Ballard, B. C. Barlaam, M. D. Hickinson, J. G. Kettle, D. J. Ogilvie, C. B. Trigwell, *Biorg. Med. Chem. Lett.* **2008**, *18*(*3*), 959.
[8] I. H. Eissa, H. Mohammad, O. A. Qassem, W. Younis, T. M. Abdelghany, A. Elshafeey, M. M. A. R. Moustafa, M. N. Seleem, A. S. Mayhoub, *J. Med. Chem.* **2017**, *130*, 73.
[9] L. F. Liu, *Annu. Rev. Biochem.* **1989**, *58*(*1*), 351.
[10] T. D. Shenkenberg, D. D. von Hoff, *Ann. Intern. Med.* **1986**, *105*(*1*), 67.
[11] C. Laurence, K. A. Brameld, J. Graton, J.-Y. Le Questel, E. Renault, *J. Med. Chem.* **2009**, *52*(*14*), 4073.
[12] C. Fraser, J. C. Dawson, R. Dowling, D. R. Houston, J. T. Weiss, A. F. Munro, M. Muir, L. Harrington, S. P. Webster, M. C. Frame, *J. Med. Chem.* **2016**, *59*(*10*), 4697.
[13] S. M. El-Moghazy, R. F. George, E. E. A. Osman, A. A. Elbatrawy, M. Kissova, A. Colombo, E. Crespan, G. Maga, *Eur. J. Med. Chem.* **2016**, *123*, 1.
[14] I. H. Eissa, A. M. El-Naggar, M. A. El-Hashash, *Bioorg. Chem.* **2016**, *67*, 43.
[15] E. Baldwin, N. Osheroff, *Curr. Med. Chem. Anticancer Agents* **2005**, *5*(*4*), 363.
[16] P.-H. Li, H. Jiang, W.-J. Zhang, Y.-L. Li, M.-C. Zhao, W. Zhou, L.-Y. Zhang, Y.-D. Tang, C.-Z. Dong, Z.-S. Huang, *Eur. J. Med. Chem.* **2018**, *145*, 498.
[17] M. Sathish, B. Kavitha, V. L. Nayak, Y. Tangella, A. Ajitha, S. Nekkanti, A. Alarifi, N. Shankaraiah, N. Nagesh, A. Kamal, *Eur. J. Med. Chem.* **2018**, *144*, 557.
[18] M. S. Christodoulou, M. Zarate, F. Ricci, G. Damia, S. Pieraccini, F. Dapiaggi, M. Sironi, L. L. Presti, A. N. García-Argáez, L. Dalla Via, D. Passarella, *Eur. J. Med. Chem.* **2016**, *118*, 79.
[19] M. S. Christodoulou, F. Calogero, M. Baumann, A. N. García-Argáez, S. Pieraccini, M. Sironi, F. Dapiaggi, R. Bucci, G. Broggini, S. Gazzola, *Eur. J. Med. Chem.* **2015**, *92*, 766.
[20] A. Kamal, M. Sathish, V. L. Nayak, V. Srinivasulu, B. Kavitha, Y. Tangella, D. Thummuri, C. Bagul, N. Shankaraiah, N. Nagesh, *Biorg. Med. Chem.* **2015**, *23*(*17*), 5511.
[21] B.-L. Yao, Y.-W. Mai, S.-B. Chen, H.-T. Xie, P.-F. Yao, T.-M. Ou, J.-H. Tan, H.-G. Wang, D. Li, S.-L. Huang, *Eur. J. Med. Chem.* **2015**, *92*, 540.
[22] M. S. Christodoulou, N. Fokialakis, D. Passarella, A. N. García-Argáez, O. M. Gia, I. Pongratz, L. Dalla Via, S. A. Haroutounian, *Biorg. Med. Chem.* **2013**, *21*(*14*), 4120.
[23] C. Bailly, *Chem. Rev.* **2012**, *112*(*7*), 3611.
[24] N. Ferri, T. Radice, M. Antonino, E. M. Beccalli, S. Tinelli, F. Zunino, A. Corsini, G. Pratesi, E. M. Ragg, M. L. Gelmi, *Biorg. Med. Chem.* **2011**, *19*(*18*), 5291.
[25] Y. Pommier, E. Leo, H. Zhang, C. Marchand, *Chem. Biol.* **2010**, *17*(*5*), 421.
[26] N. Ferri, E. M. Beccalli, A. Contini, A. Corsini, M. Antonino, T. Radice, G. Pratesi, S. Tinelli, F. Zunino, M. L. Gelmi, *Biorg. Med. Chem.* **2008**, *16*(*4*), 1691.
[27] D. R. Romer, *J. Heterocycl. Chem.* **2009**, *46*(*2*), 317.
[28] G. Minotti, P. Menna, E. Salvatorelli, G. Cairo, L. Gianni, *Pharmacol. Rev.* **2004**, *56*(*2*), 185.
[29] J. Gallego, A. R. Ortiz, B. de Pascual-Teresa, F. Gago, *J. Comput.-Aided Mol. Des.* **1997**, *11*(*2*), 114.
[30] S. A. Bailey, D. E. Graves, R. Rill, *Biochemistry* **1994**, *33*(*38*), 11493.

[31] Z. Li, J.-H. Tan, J.-H. He, Y. Long, T.-M. Ou, D. Li, L.-Q. Gu, Z.-S. Huang, *Eur. J. Med. Chem.* **2012**, *47*, 299.
[32] J.-H. He, H.-Y. Liu, Z. Li, J.-H. Tan, T.-M. Ou, S.-L. Huang, L.-K. An, D. Li, L.-Q. Gu, Z.-S. Huang, *Eur. J. Med. Chem.* **2013**, *63*, 1.
[33] H.-Q. Zhang, F.-H. Gong, C.-G. Li, C. Zhang, Y.-J. Wang, Y.-G. Xu, L.-P. Sun, *Eur. J. Med. Chem.* **2016**, *109*, 371.
[34] D. Goff, J. Zhang, T. Heckrodt, J. Yu, P. Ding, R. Singh, S. Holland, W. Li, M. Irving, *Biorg. Med. Chem. Lett.* **2017**, *27*(*16*), 3766.
[35] A. Rescifina, C. Zagni, M. G. Varrica, V. Pistarà, A. Corsaro, *Eur. J. Med. Chem.* **2014**, *74*, 95.
[36] G. Marzaro, L. Dalla Via, A. Toninello, A. Guiotto, A. Chilin, *Biorg. Med. Chem.* **2011**, *19*(*3*), 1197.
[37] C.-M. Cheng, Y.-J. Lee, W.-T. Wang, C.-T. Hsu, J.-S. Tsai, C.-M. Wu, K.-L. Ou, T.-S. Yang, *Res. Commun.* **2011**, *404*(*1*), 297.
[38] N. Shankaraiah, C. Jadala, S. Nekkanti, K. R. Senwar, N. Nagesh, S. Shrivastava, V. Naidu, M. Sathish, A. Kamal, *Biorg. Chem.* **2016**, *64*, 42.
[39] B. A. Dar, A. M. Lone, W. A. Shah, M. A. Qurishi, *Eur. J. Med. Chem.* **2016**, *111*, 26.
[40] T. K. Venkatachalam, P. V. Bernhardt, C. J. Noble, N. Fletcher, G. K. Pierens, K. J. Thurecht, D. C. Reutens, *J. Inorg. Biochem.* **2016**, *162*, 295.
[41] A. M. El-Naggar, M. M. Abou-El-Regal, S. A. El-Metwally, F. F. Sherbiny, I. H. Eissa, *Mol. Divers.* **2017**, *21*(*4*), 967.
[42] W. M. Eldehna, M. F. Abo-Ashour, A. Nocentini, P. Gratteri, I. H. Eissa, M. Fares, O. E. Ismael, H. A. Ghabbour, M. M. Elaasser, H. A. Abdel-Aziz, *Eur. J. Med. Chem.* **2017**, *139*, 250.
[43] A. M. El-Naggar, I. H. Eissa, A. Belal, A. A. El-Sayed, *RSC Adv.* **2020**, *10*(*5*), 2791.
[44] H. A. Mahdy, M. K. Ibrahim, A. M. Metwaly, A. Belal, A. B. Mehany, K. M. El-Gamal, A. El-Sharkawy, M. A. Elhendawy, M. M. Radwan, M. A. Elsohly, *Biorg. Chem.* **2020**, *94*, 103422.
[45] A. G. A. El-Helby, H. Sakr, I. H. Eissa, A. A. Al-Karmalawy, K. El-Adl, *Arch. Pharm.* **2019**, *352*(*12*), e1900178.
[46] A. G. A. El-Helby, H. Sakr, I. H. Eissa, H. Abulkhair, A. A. Al-Karmalawy, K. El-Adl, *Arch. Pharm.* **2019**, *352*(*10*), e1900113.
[47] S. A. Elmetwally, K. F. Saied, I. H. Eissa, E. B. Elkaeed, *Bioorg. Chem.* **2019**, *88*, 102944.
[48] A. A. Gaber, A. H. Bayoumi, A. M. El-morsy, F. F. Sherbiny, A. B. Mehany, I. H. Eissa, *Bioorg. Chem.* **2018**, *80*, 375.
[49] I. H. Eissa, A. M. El-Naggar, N. E. El-Sattar, A. S. Youssef, *Curr. Med. Chem. Anticancer Agents* **2018**, *18*(*2*), 195.
[50] M. Ibrahim, M. Taghour, A. Metwaly, A. Belal, A. Mehany, M. Elhendawy, M. Radwan, A. Yassin, N. El-Deeb, E. Hafez, *Eur. J. Med. Chem.* **2018**, *155*, 117.
[51] I. H. Eissa, A. M. Metwaly, A. Belal, A. B. Mehany, R. R. Ayyad, K. El-Adl, H. A. Mahdy, M. S. Taghour, K. M. El-Gamal, M. E. El-Sawah, *Arch. Pharm.* **2019**, *352*(*11*), e1900123.
[52] N. Jiang, X. Zhai, Y. Zhao, Y. Liu, B. Qi, H. Tao, P. Gong, *Eur. J. Med. Chem.* **2012**, *54*, 534.
[53] D. Shah, H. Lakum, K. Chikhalia, *Russ. J. Bioorg. Chem.* **2015**, *41*(*2*), 209.
[54] M. M. Gineinah, M. Nasr, A. Abdelal, A. El-Emam, S. Said, *Med. Chem. Res.* **2000**, *10*(*4*), 243.
[55] F. Kathawala, Google Patents, United States, US3847918A, **1974**.
[56] T. Mosmann, *J. Immunol. Methods* **1983**, *65*(*1–2*), 55.
[57] F. Denizot, R. Lang, *J. Immunol. Methods* **1986**, *89*(*2*), 271.
[58] M. Thabrew, R. D. Hughes, I. G. Mcfarlane, *J. Pharm. Pharmacol.* **1997**, *49*(*11*), 1132.
[59] P. Furet, G. Caravatti, N. Lydon, J. P. Priestle, J. M. Sowadski, U. Trinks, P. Traxler, *J. Comput.-Aided Mol. Des.* **1995**, *9*(*6*), 465.
[60] N. S. Burres, A. Frigo, R. R. Rasmussen, J. B. McAlpine, *J. Nat. Prod.* **1992**, *55*(*11*), 1582.
[61] S. Maddika, S. R. Ande, S. Panigrahi, T. Paranjothy, K. Weglarczyk, A. Zuse, M. Eshraghi, K. D. Manda, E. Wiechec, M. Los, *Drug Resist. Update* **2007**, *10*(*1–2*), 13.
[62] F. Bunz, *Curr. Opin. Pharmacol.* **2001**, *1*(*4*), 337.
[63] K. K.-W. Lo, T. K.-M. Lee, J. S.-Y. Lau, W.-L. Poon, S.-H. Cheng, *Inorg. Chem.* **2008**, *47*(*1*), 200.
[64] H. Patel, K. Dhangar, Y. Sonawane, S. Surana, R. Karpoormath, N. Thapliyal, M. Shaikh, M. Noolvi, R. Jagtap, *Arab. J. Chem.* **2015**, *11*(*2*), 221.
[65] M.-K. Ibrahim, A. A. Abd-Elrahman, R. R. Ayyad, K. El-Adl, A. M. Mansour, I. H. Eissa, *Bull. Fac. Pharm., Cairo Univ.* **2013**, *51*(*1*), 101.
[66] S. Léonce, V. Pérez, S. Lambel, D. Peyroulan, F. Tillequin, S. Michel, M. Koch, B. Pfeiffer, G. Atassi, J. A. Hickman, *Mol. Pharmacol.* **2001**, *60*(*6*), 1383.

SUPPORTING INFORMATION

Additional Supporting Information may be found online in the supporting information tab for this article.

How to cite this article: Alesawy MS, Al-Karmalawy AA, Elkaeed EB, et al. Design and discovery of new 1,2,4-triazolo [4,3-*c*]quinazolines as potential DNA intercalators and topoisomerase II inhibitors. *Arch Pharm.* 2020;e2000237. https://doi.org/10.1002/ardp.202000237